

Brain Microstructure Mapping from diffusion MRI using Least Squares Variable Separation

Hamza Farooq¹, Junqian Xu², Essa Yacoub³, Tryphon Georgiou¹, and
Christophe Lenglet³

¹ Electrical and Computer Engineering Dept, University of Minnesota, United States

² Department of Radiology, Icahn School of Medicine, The Mount Sinai Hospital,
New York, United States

³ Center for Magnetic Resonance Research, Department of Radiology, University of
Minnesota, United States

Abstract. We introduce a novel data fitting procedure of multicompartment models for diffusion MRI (dMRI) data of the brain white matter. These biophysical models aim to characterize important microstructure quantities like axonal radius, density and orientations. In order to describe the underlying tissue properties, a variety of models for intra-/extra-axonal diffusion signals have been proposed. Combinations of these analytic models are used to predict the diffusion MRI signal in multi-compartment settings. However, parameter estimation from these multi-compartment models is an ill-posed problem. Consequently, many existing fitting algorithms either rely on an initial brute force grid search to find a good start point, or have strong assumptions like single fiber orientation to estimate some of these parameters from simpler models like the diffusion tensor (DT). In both cases, there is a tradeoff between computational complexity and accuracy of the estimated parameters. Here, we describe a novel algorithm based on the separation of the Nonlinear Least Squares (NLLS) fitting problem, via Variable Projection Method, to search for nonlinearly and linearly entering parameters independently. We use stochastic global search algorithms to find a global minimum, while estimating nonlinearly entering parameters. The approach is independent of any starting point, and does not rely on estimates from simpler models. We show that the suggested algorithm is faster than algorithms involving grid search, and its greater accuracy and robustness are demonstrated on synthetic as well as real data.

1 Introduction

Diffusion MRI can measure (water) molecules displacement in a certain time interval within a structure. This can be used to reveal tissue micro structure information using biophysical tissue models. Simplest of these models is Diffusion Tensor [1], giving simple bio-markers like Mean Diffusivity (MD) and Fractional Anisotropy (FA). However, more specific markers like axon radius, density and volume fractions of different compartments can be estimated from sophisticated multi compartment models, as suggested for example in [2] and [3].

The problem of fitting diffusion MRI data to these biophysical models is not well posed due to the type of functions or models describing diffusion in a certain geometry. These functions depend non linearly on variables to be estimated and over-all problem is non-convex, thus having many local optima. Any optimization algorithm using gradient based methods will largely depend upon a good starting point to reach global optimum.

Initial grid search over physically possible range of parameters is done in NODDI [2] and ActiveAx [3] to get a starting point for solving Gauss-Newton (GN) nonlinear optimization problem for parameter estimation. CAMINO [4] uses estimates from simpler models to provide initial estimates to complex multi compartment models. Resultantly, before solving a three compartment model using Levenberg Marquardt (LM) method, CAMINO may solve approximately four simpler models to have an initial guess. Grid search and estimates from simpler models, increase the possibility of reaching global optimum but add to computational complexity and estimation time. AMICO [5] presents multi compartment models (as suggested in [2] and [3]) parameter estimation as a convex problem. The problem is viewed as convex by estimating fiber orientation from DT model and then searching for linearly entering parameters only, over a grid or dictionary of remaining two nonlinearly entering parameters. The approach converges very fast but needs to be adapted in the presence of three or more non linearly entering parameters. All estimation algorithms discussed above assume single, known fiber orientation in a voxel. CAMINO and AMICO rely on this assumption for further estimation of remaining parameters.

This study aims to suggest an algorithm for estimating multi compartment brain tissue models parameters without using initial grid search over the whole parameter range and also without using simpler models for initial estimation. Rather, problem has been approached by separating linear and nonlinearly entering parameters. Suggested method converges twice as fast as CAMINO mainly due to Variable Projection and stochastic global search algorithms to find global minimum in nonlinear parameters estimation. Suggested algorithm has been tested with both synthetic data generated by CAMINO and real MRI data. Results show excellent fitting performance on all data sets and in the presence of Rician noise.

2 Problem Formulation

Typical estimation problem of multicompartment tissue model parameters from diffusion MRI data in the presence of offset Gaussian noise [8] is of the following form:

$$\min_{x, f} \sum_{k=1}^N \sigma^{-2} (y(k) - \sum_{i=1}^n \sqrt{f_i e^{A_i(x)} + \sigma^2})^2 \quad (1)$$

where y represents normalized MRI measurements and N is the total number of measurements available. $f = [f_1 \ f_2 \ \dots \ f_n]'$ is vector containing volume

fractions of n compartments. $x = [x_1 \ x_2 \ \dots \ x_m]'$ is vector containing m parameters on which functions describing diffusion in n compartments depend upon. $A_1, A_2 \dots A_n$ are chosen as per selected models for Intra-Axonal compartment, Extra-Axonal compartment, cerebrospinal fluid (CSF) compartment and glial cells etc. σ is standard deviation of noise which is calculated before hand from b_0 measurements of MRI. σ adds a constant bias to measurements and can easily be taken care of. By dropping σ , we can rewrite objective function in (1) including constraints as following:

$$\min_{x, f} \| y - (f_1 e^{-A_1(x_1, \dots, x_{m1})} + f_2 e^{-A_2(x_{m1+1}, \dots, x_{m2})} + \dots + f_n e^{-A_n(x_{m2+1}, \dots, x_m)}) \|_2^2 \quad (2)$$

$$\begin{aligned} \text{such that} \quad & \sum_{i=1}^n f_i = 1 \\ & f_i \geq 0 \quad i = 1, 2 \dots n \\ & lb_j \leq x_j \leq ub_j \quad j = 1, 2 \dots m \end{aligned}$$

where lb and ub represent lower bound and upper bound for unknown deterministic variables x . Variables in x will vary with each choice of multicompartment model. Known parameters in x have been described in supplementary material.

3 Suggested Algorithm

Detail of suggested algorithm is given in following four steps.

- **Step 1. Variable Projection for Separating Non Linearly Entering Parameters.** We can exploit separable structure of the problem described in eq (1) by variable separation method as suggested in [6]. We can re-write our objective function as in (1) in following form:

$$\begin{aligned} & \min_{x, f} \| y - \Phi(x)f \|_2^2 \\ & \text{where } f = [f_1 \ f_2 \ \dots \ f_n]' \\ \text{and } \Phi(x) = & [e^{-A_1(x_1, \dots, x_{m1})} \ e^{-A_2(x_{m1+1}, \dots, x_{m2})} \ \dots \ e^{-A_n(x_{m2+1}, \dots, x_m)}] \end{aligned} \quad (3)$$

For any estimate of 'x', linear parameters 'f' can be calculated from linear least squares as below:

$$f = \Phi^\dagger(x)y \quad (4)$$

where $\Phi^\dagger(x)$ is Moore-Penrose inverse of $\Phi(x)$

$$\text{i.e., } \Phi^\dagger(x) = (\Phi(x)^T \Phi(x))^{-1} \Phi(x)^T \quad (5)$$

by substituting (5) in (3), our objective function takes following form:

$$\min_x \| y - \Phi(x)(\Phi(x)^T \Phi(x))^{-1} \Phi(x)^T y \|_2^2 \quad (6)$$

$$\min_x \| (I - \Phi(x)(\Phi(x)^T \Phi(x))^{-1} \Phi(x)^T) y \|_2^2 \quad (7)$$

(7) is called the variable projection functional. With an assumption of $\Phi(x)$ to have a locally constant rank, it has been proven in [6] that global minimum of (7) remains the same as global minimum in (3).

- **Step 2. Non Linear Parameters Estimation by Genetic Algorithm (GA).** It has been shown in [9] that GA can be used efficiently for NLLS estimation of 'x' for problems of the form (7). Elitism based approach was used with population size of 24 to 40. Stopping criteria of 70 to 100 generations was found sufficient for convergence in this problem setting. For implementing GA, toolbox developed by University of Sheffield, and available freely at university website¹ was used.
- **Step 3. Constrained Linear Parameters Estimation.** Once nonlinear parameters x are known, estimation of linear parameters is a linear least squares estimation problem as shown in (4).
- **Step 4. NLLS Estimation Using Gradient Based Methods.** Estimates after step 3 are fairly accurate however, we can refine the results using gradient based methods (for example MATLAB's 'lsqcurvefit') by constrained NLLS estimation. Also we can reduce number of iteration of GA by employing this step.

4 Results

4.1 Analysis Using Synthetic Data

Suggested algorithm has been tested with synthetic data generated by open source software CAMINO [4] using 'datasynth'. Comparison of results can be shown for following example where data was generated using 'ZepplinCylinderDot' model with Rician noise at different SNR.

Example Problem - dMRI Data Fitting to 'ZepplinCylinderDot'

$$\min_{R, \theta, \phi, d_{\perp}, f} \| y - (f_1 e^{-A_{cylinder}(R, \theta, \phi)} + f_2 e^{-A_{Zepplin}(\theta, \phi, d_{\perp})} + f_3 e^{-A_{Dot}}) \|_2^2 \quad (8)$$

$$\text{such that } \sum_{i=1}^3 f_i = 1, \quad f_i \geq 0 \quad i = 1, 2, 3.$$

$$0 \leq R \leq 20, \quad 0 \leq \theta \leq 2\pi, \quad 0 \leq \phi \leq \pi$$

$$d_{\perp} = d_{\parallel} (1 - (f_1 / (f_1 + f_2)))$$

$$\text{Fibre direction vector } n = [\cos \phi \sin \theta \quad \sin \phi \sin \theta \quad \cos \theta] \quad (9)$$

For simplicity only unknown parameters have been shown in (8) and described as following. f_1, f_2 and f_3 are Intra-Axonal, Extra-Axonal and CSF compartment volume fractions. d_{\parallel} (diffusion coefficient in parallel to fiber orientation, fixed for in-vivo) = $1.7e^{+3}$ ($\text{sec}/\mu\text{m}^2$), d_{\perp} ($\text{sec}/\mu\text{m}^2$) is diffusion coefficient

¹ <http://codem.group.shef.ac.uk/index.php/ga-toolbox>

in perpendicular to fiber orientation. Constraint given in (8) on d_{\perp} , is from a simple tortuosity model given in [10]. Axon Radius (average) = R (μm) while θ (rad) and ϕ (rad) give fiber orientation as in (9). Detail of functions describing $e^{-A_{cylinder}}$, $e^{-A_{zeppelin}}$ and $e^{-A_{dot}}$ can be found in [7].

Objective Function Analysis . Having synthetic data generated, objective function given in (8) can be visualized by plotting with assumption of only two unknowns at a time. Some of the plots are shown in Fig. 1. It can be seen in Fig. 1 (A) and (C) that if θ is constrained as in (8), there can be two distinct solutions for n (180° apart). Fig. 1 (C) shows that if any gradient based method is used, and initial value of R is greater than a certain point (depending upon true value of R), solution can never converge to global minimum. This also explains difficulty in detection of small R values. Fig. 2 shows effect of Rician noise on objective function. It can be seen that a constant bias is increased with more noisy signal.

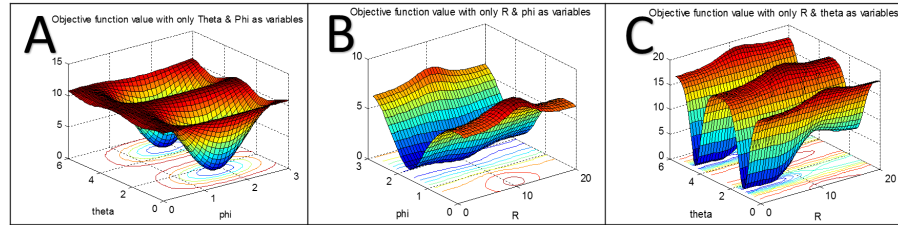


Fig. 1: Objective Function Plots when, (A) θ and ϕ , (B) R and ϕ , (C) R and θ , are only variables in each case.

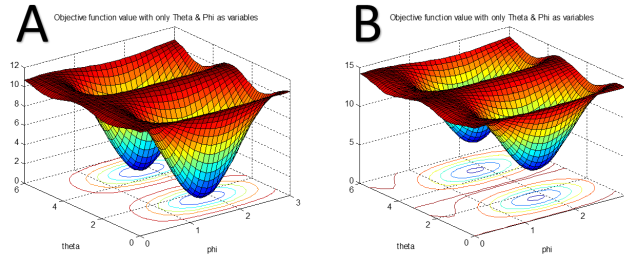


Fig. 2: Objective Function Plot at (A) SNR =200, (B) SNR =12 for θ and ϕ as only variables.

Comparison of Results with CAMINO. For all parameter estimates and at all SNR levels, suggested method shows 100 percent success ratio on synthetic data, which is not the case in CAMINO. Fig. 3 - Fig. 6 show estimated parameters histograms for 100 runs at SNR = 25. Model fitting was done in CAMINO using 'modelfit' with 'MULTIRUNLM' (100 iterations). R and orientation estimates are not effected by noise using suggested method. However, R is underestimated by $0.04 - 0.05\mu m$ at all SNR levels.

6

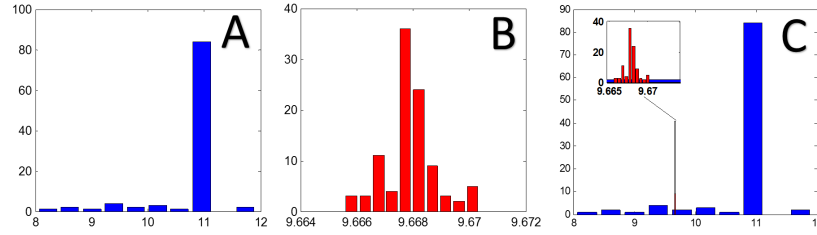


Fig. 3: Histogram of Axon Radius estimates using synthetic data SNR=25 with True Value of $R = 10 \mu m$ (A) CAMINO ($8 - 12 \mu m$) (B) Proposed Algorithm ($9.66 - 9.67 \mu m$) (C) Histograms Superimposed

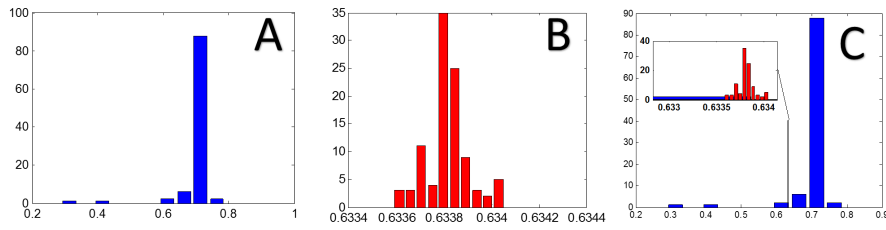


Fig. 4: Histogram of $v = f_1/(f_1 + f_2)$ estimates using synthetic data SNR=25 with True Value of $v = 0.7$ (A) CAMINO ($0.3 - 0.8$) (B) Proposed Algorithm ($0.633 - 0.634$) (C) Histograms Superimposed

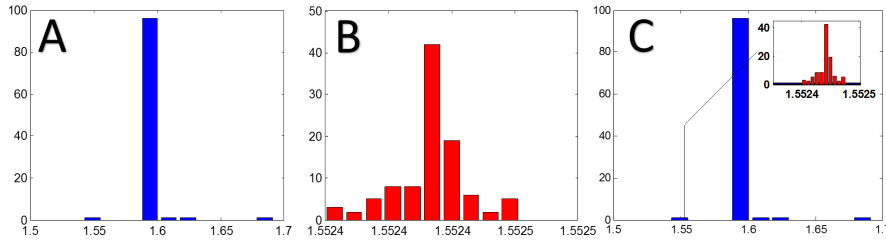


Fig. 5: Histogram of θ estimates using synthetic data SNR=25 with True Value of $\theta = 1.54 \text{ rad}$ (A) CAMINO ($1.5 - 1.7$) (B) Proposed Algorithm ($1.5524 - 1.5525$) (C) Histograms Superimposed

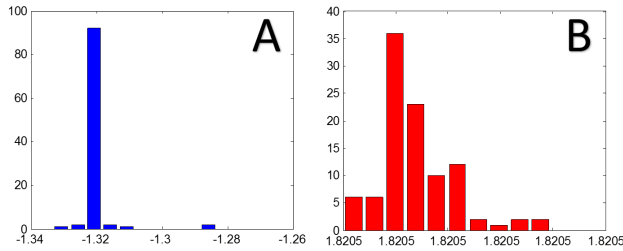


Fig. 6: Histogram of ϕ estimates using synthetic data SNR=25 with True Value of $\phi = 1.83 \text{ rad}$ (A) CAMINO ($-1.43 - 1.26$) (B) Proposed Algorithm ($1.8205 - 1.8205$)

Time Complexity. Estimation time depends upon number of measurements. In case of CAMINO it also increases with noisy data. For this example fitting time (per voxel) for CAMINO varied from 10 - 13 seconds while suggested method took 4.8 seconds at the most. Time was calculated without any parallel processing on a same machine (corei7 with 12 GB RAM).

4.2 Analysis Using Real MRI Data

Results Using Ex Vivo Monkey Brain Data. Fixed monkey brain data set¹ as used in [2], was used to compare results with CAMINO. Data was fit in CAMINO using 'mmwmdfixed' model as shown in CAMINO website². Four compartment model ('Zeppelin Cylinder Ball Dot') as suggested in [2] was used to estimate parameters using suggested algorithm. Fig. 4 shows radius estimates comparison while Fig. 5 shows Density Index (ρ') = $f_1/(f_1 + f_2)\pi R^2$ estimates comparison for mid-sagittal slice of Corpus Callosum (CC).

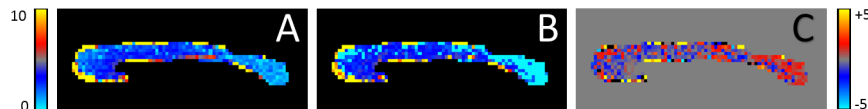


Fig. 7: Results for ex vivo monkey brain data (A) Radius estimates by CAMINO (B) Radius estimates by Suggested Algorithm (C) Difference (all units in μm)

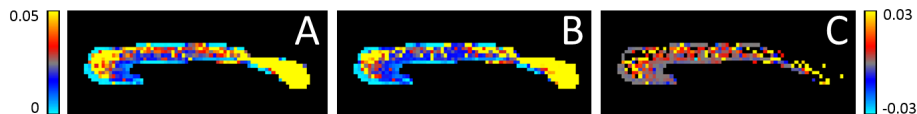


Fig. 8: Results for ex vivo monkey brain data (A) ρ' estimates by CAMINO (B) ρ' estimates by Suggested Algorithm (C) Difference

Ex-vivo Data Results. Results exhibit identical pattern throughout CC i.e., densely packed small axon radii in genu and splenium while larger axon radii with less density in mid-body. However, CAMINO over estimates axon radii in both genu and splenium region (by around $3 \mu m$) and under estimates radii in mid-body (by around $2 \mu m$) as compared to suggested method. Density index is over estimated in mid-body and under-estimated in genu and splenium region by CAMINO as compared to suggested method.

Results Using In Vivo Human Brain Data

Data Acquisition. Diffusion MRI data was acquired on a healthy volunteer using a Siemens 3T Skyra system with voxel size $2 \times 2 \times 2 mm$, and four b-values, each with 119 directions and 18 additional b=0 volumes.

¹ <http://dig.drcomr.dk/activeax-dataset/>

² <http://cmic.cs.ucl.ac.uk/camino/index.php?n=Tutorials.ActiveAx>

Data Fitting. Data was fitted in CAMINO using 'mmwmdin vivo' model. For suggested method, three compartment model 'Zeppelin Cylinder Ball' (neglecting stationary compartment for in-vivo as suggested in [2]) was used. Fig. 6 shows radius estimates, while Fig. 7 shows ρ' estimates comparison for CC .

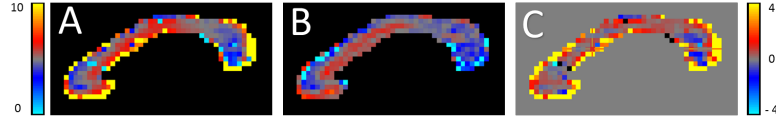


Fig. 9: Results for in-vivo human brain data (A) Radius estimates by CAMINO (B) Radius estimates by Suggested Algorithm (C) Difference (all units in μm)

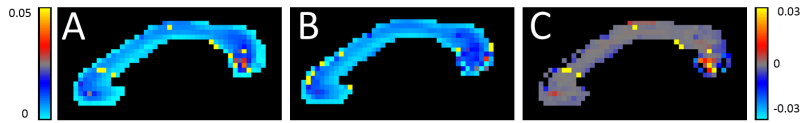


Fig. 10: Results for in-vivo human brain data (A) ρ' estimates by CAMINO (B) ρ' estimates by Suggested Algorithm (C) Difference

In-vivo Data Results. Results are generally in close match for both methods. However, CAMINO is over estimating radii in genu outer region, while underestimating in splenium inner region.

5 Discussion

Suggested dMRI data fitting method can be used without any modification to all multicompartment models discussed in [7]. It has been shown that the method is faster and reliable than any other method involving grid search and Markov Chain Monte Carlo (MCMC). It does not rely on any assumption like single fiber orientation, and directly estimates multicompartment parameters from given dMRI data, independent of any initial guess.

Acknowledgments. Work partly supported by NIH grants P41 EB015894, P30 NS076408 the Human Connectome Project (U54 MH091657) and Fulbright Program.

References

1. Basser, J. P., Mattiello, J., LeBihan, D.: MR diffusion tensor spectroscopy and imaging Biophys. J., **66**, 259–267 (1994)
2. Zhang, H., Schneider, T., Wheeler-Kingshott, C.A.M., Alexander, D.C.: NODDI: Practical in vivo orientation dispersion and density imaging of the human brain. NeuroImage **61**, 1000–1016 (2012)

3. Alexander, D.C., Hubbard, P.L., Hall, M.G., Moore, E.A., Ptito, M., Parker, G.J., Dyrby, T.B.: Orientationally invariant indices of axon diameter and density from diffusion MRI *Neuroimage.*, **52**, 1374-89 (2010)
4. Cook, P. A., Bai, Y., Nedjati-Gilani, S., Seunarine, K. K., Hall, M. G., Parker, G. J., Alexander, D. C.: Camino: Open-Source Diffusion-MRI Reconstruction and Processing, 14th Scientific Meeting of the International Society for Magnetic Resonance in Medicine, Seattle, WA, USA, p. 2759, May 2006.
5. Daducci, A., Canales-Rodríguez, E., Zhang, H., Durby, T., Alexander, D.C., Thiran J.P.: Accelerated Microstructure Imaging via Convex Optimization (AMICO) from Diffusion MRI data. *NeuroImage* **105**, 32-44 (2015)
6. Golub, G. H., and Pereyra V.: The differentiation of pseudo-inverses and nonlinear least squares problems whose variables separate *SIAM J. Numer. Anal.* **10** 413-432 (1973)
7. Panagiotaki, E., Schneider, T., Siow, B., Hall M. G., Lythgoe M.F., Alexander, D.C.: Compartment models of the diffusion MR signal in brain white matter: A taxonomy and comparison. *NeuroImage* **59**, 2241-2254 (2012)
8. Alexander, D. C.: Modelling, fitting and Sampling of Diffusion MRI. *Visualization and Processing of Tensor Field*, 3-20 (2009)
9. Mitra, S., Mitra, A.: A genetic algorithms based technique for computing the non-linear least squares estimates of parameters of sum of exponentials model. *Expert systems with Applications* **39**, 6370-6379 (2012)
10. Szafer, A., Zhong, J., Gore, J.C.: Theoretical model for water diffusion in tissues. *Magn. Reson. Med.* **33**, 697-712, (1995)